# Search for octupole correlations in neutron-rich $^{148}$Ce nucleus

Y. J. Chen,[1] S. J. Zhu,[1,2,*] J. H. Hamilton,[2] A. V. Ramayya,[2] J. K. Hwang,[2] M. Sakhaee,[1] Y. X. Luo,[2,3] J. O. Rasmussen,[3]
K. Li,[2] I. Y. Lee,[3] X. L. Che,[1] H. B. Ding,[1] and M. L. Li[1]

[1]*Department of Physics, Tsinghua University, Beijing 100084, People's Republic of China*
[2]*Department of Physics, Vanderbilt University, Nashville, Tennessee 37235, USA*
[3]*Lawrence Berkeley National Laboratory, Berkeley, California 94720, USA*

New transitions and levels in $^{148}$Ce have been observed in a $\gamma$-$\gamma$-$\gamma$ coincidence study from the spontaneous fission of $^{252}$Cf with Gammasphere detector array. The ground band has been extended up to $I^{\pi} = 22^{+}$, and side bands are extended with $\Delta I = 2$ stretched transitions and $\Delta I = 1$ crossing transitions. The observed level scheme is interpreted in terms of possible octupole correlations. Two sets of interwined positive- and negative-parity bands with the simplex quantum numbers $s = \pm 1$ are suggested. The results of $B(E1)/B(E2)$ branching ratios indicate that the octupole correlations in $^{148}$Ce are strong.

## I. INTRODUCTION

Theoretical calculations in the deformed shell model have predicted the existence of an island of octupole correlated nuclei with reflection asymmetric shape with proton numbers near 56 and neutron numbers near 88 [1–3]. In such nuclei, the level patterns are similar to rotational bands observed in reflection-asymmetric molecules including two bands of parity doublets characterized with simplex quantum numbers [4] $s = \pm 1$ and $s = \pm i$. The positive- and negative-parity rotational bands are interwined by strong $E1$ transitions [1]. For even-even nuclei, the spins and parities ($I^{\pi}$'s) of the levels in an octupole deformation band are $I^{\pi} = 0^{+}, 1^{-}, 2^{+}, 3^{-}, \ldots$ for the $s = +1$ band, and $I^{\pi} = 0^{-}, 1^{+}, 2^{-}, 3^{+}, \ldots$ for the $s = -1$ band. For odd-$A$ nuclei, $I^{\pi} = 1/2^{+}, 3/2^{-}, 5/2^{+}, 7/2^{-}, \ldots$ for the $s = +i$ band, and $I^{\pi} = 1/2^{-}, 3/2^{+}, 5/2^{-}, 7/2^{+}, \ldots$ for the $s = -i$ band.

The presence of octupole deformation around $Z = 56, N = 88$ has been confirmed in $^{140-146}$Ba [5–9], $^{144,146}$Ce [5,10,11], and $^{145,147}$La [12,13] by measuring the prompt $\gamma$ rays from spontaneous fission of actinide nuclei. For odd-$A$ nuclei in this region, the $s = \pm i$ bands of parity doublets have been observed in $^{145}$La [12,13] and $^{143,145}$Ba [7,8]. For even-even nuclei, the ground state $s = +1$ band has been observed in a number of nuclei [14], but the $s = -1$ band was only reported in $^{148}$Sm [15] and $^{146}$Nd [16]. In Ce and Ba isotopes, only the $s = +1$ band has been observed [5–11]. Therefore, searching for the $s = -1$ band in this region and extending already known $s = +1$ bands to higher spin can provide useful information for nuclear structure studies.

The level structures of $^{144,146}$Ce [6,10,11] show evidence for octupole deformation. The levels in $^{144,146}$Ce have several intertwined $E1$ transitions between the two branches of the $s = +1$ band of parity doublets. These features are similar to those observed in $^{142,144,146}$Ba nuclei [6,9] with the $s = +1$ band structure. In the cranked shell model calculations [17,18], the nucleus $^{148}$Ce is predicted to show strong octupole

correlations. In an earlier publication [10], $^{148}$Ce had significantly different structure from those of $^{144,146}$Ce, because there was no evidence of a negative-parity band with $E1$ transitions intertwined with the yrast cascade. Urban *et al.* [19] reported octupole correlations in $^{148}$Ce only in terms of an experimental electric dipole moment value, but no collective band was given. In our earlier publication [5], we showed our initial level scheme of $^{148}$Ce in an experiment carried out with the 36 Ge detectors in the early implementation stage of Gammasphere, but with no detailed discussion.

In the present work, we investigate the band structures of $^{148}$Ce by studying the $\gamma$ rays emitted by the fragments from the spontaneous fission of $^{252}$Cf, in order to extend the levels of $^{148}$Ce and to search for evidence of octupole correlations. In particular, it is of interest to search for the $s = \pm 1$ bands, and to compare the level systematics of $^{148}$Ce with those of $^{144}$Ce and $^{146}$Ce. New band structures are observed in $^{148}$Ce and are connected by intertwined $E1$ transitions. These band structures are interpreted as the bands of parity doublets with $s = \pm 1$ related to possible octupole correlations.

## II. EXPERIMENTS AND RESULTS

The $^{148}$Ce nucleus was studied by measuring the prompt $\gamma$ rays from spontaneous fission of $^{252}$Cf. The experiment was carried out at the Lawrence Berkeley National Laboratory using a $^{252}$Cf source of about 60 $\mu$Ci. The source was sandwiched between two Fe foils of thickness 10 mg/cm$^2$. They were placed at the center of the Gammasphere array which, for this experiment, consisted of 102 Compton suppressed Ge detectors. The data were recorded in an event-by-event mode. A total of $5.7 \times 10^{11}$ triple- and higher-fold coincidence events were collected. These data have higher statistics than the earlier measurements of Refs. [8,13,20] by a factor of ~15 at higher energy and a factor of ~50 at lower energy (absorbers were removed). The data were analyzed with the RADWARE software package [21] using $\gamma$-$\gamma$-$\gamma$ coincidence methods. New transitions were identified and assigned in the present work by setting several double gates on known transitions in $^{148}$Ce. Newly assigned transitions were then used as gates
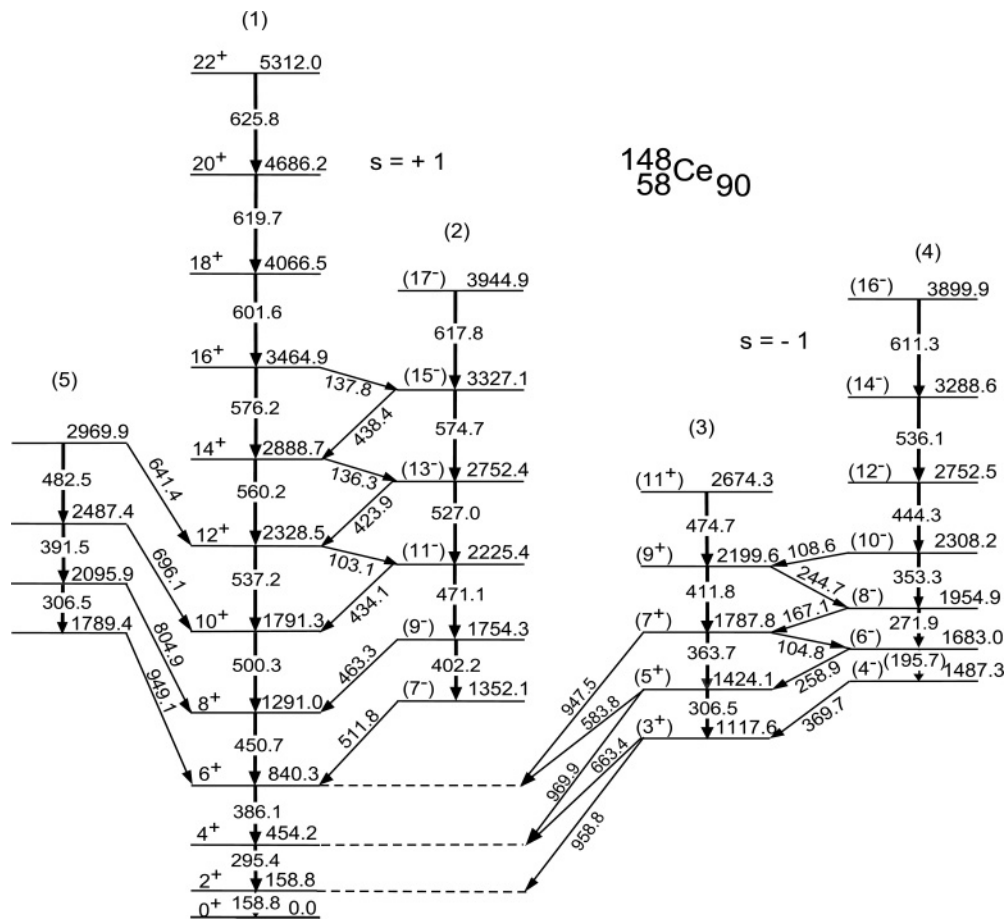
*Electronic address: zhushj@mail.tsinghua.edu.cn

FIG. 1. Partial level scheme of $^{148}$Ce. 20 new $\gamma$ transitions and nine new levels are added.

to identify additional transitions. Further experimental details can be found in Refs. [8,13,22].

The level scheme of $^{148}$Ce observed in the present work is shown in Fig. 1. 20 new transitions are observed and nine new levels are reported in the level scheme of $^{148}$Ce compared to our previous report [5]. In this work, the yrast band is extended to spin 22. In our previous work [5], the two lowest levels in band (2) and the two intermediate levels in band (5) were seen but no band structures were connected to them as seen in the present work. Band (3) is extended to spin 11 compared to our previous work [5] and the 1487.3-keV level was added to band (4) along with the 104.8-keV transition. The new structures were deduced from the $\gamma$-$\gamma$-$\gamma$ coincidence relationships, the relative transition intensity analysis and the total internal conversion coefficient analysis. The results of these analyses are given in Tables I and II, including the $\gamma$-transition energies, the relative intensities of the transitions, and the assignments of spin and parity ($I^\pi$) values. The $\gamma$-transition intensities have been normalized to that of the 295.4-keV ($4^+ \rightarrow 2^+$) $\gamma$ ray. Five collective bands with $\Delta I = 2$ stretched transitions are labeled as (1), (2), (3), (4), and (5) on the top of the scheme. Based on the regular level spacings in each band and systematic comparisons, we assigned these bands to have $\Delta I = 2$ stretched $E2$ transitions.

Figure 2 gives examples of some double-gated $\gamma$-ray spectra. In Fig. 2(a), the $\gamma$-ray spectrum is obtained by double

gating on the known 537.2- and 560.2-keV transitions of band (1). One can clearly see the known 158.8-, 295.4-, 386.1-, 450.7-, 500.3-, 576.2-, 601.6-, 619.7-keV transitions and the new 625.8-keV transition in band (1). The partner transitions 212.5- and 352.0-keV in $^{100}$Zr are also seen. In Fig. 2(b) the coincidence spectrum obtained by double gating on 295.4- and 386.1-keV transitions is shown. In this spectrum one can clearly see several strong transitions belonging to band (1), three transitions 402.2-, 471.1-, 527.0-keV belonging to band (2), and linking transitions 511.8-, 463.3-, 434.1-, 423.9-, 438.4-, 103.1-keV between bands (1) and (2). The linking transitions 804.9-, 696.1-, and 641.4-keV between bands (1) and (5), and three transitions 306.5-, 391.5-, and 482.5-keV belonging to band (5) also can be seen. Moreover, some transitions in bands (3) and (4) as well as some linking transitions between bands (3) and (4) are also observed. Figure 2(c) shows a coincidence spectrum for bands (3) and (4), with the double gated energies of 295.4- and 969.9-keV. One can clearly see 363.7-, 411.8- and 474.7-keV transitions belonging to band (3), and 271.9-, 353.3-, 444.3-, 536.1-, and 611.3-keV transitions belonging to band (4). In addition, the strong interwined transitions 104.8-, 108.6-, 167.1-, 244.7-, and 258.9-keV between bands (3) and (4) are also seen in this double-gated spectrum.

Based on systematic comparisons with neighboring nuclei $^{144,146}$Ce, we tentatively assigned the band (2) as the

TABLE I. $\gamma$-ray transition energies, the relative intensities, and the assignments of spin and parity ($I^\pi$) value for $^{148}$Ce in this work.

| $E_\gamma$(keV) | $I_i^\pi \to I_f^\pi$ | $I_\gamma$(%) | $E_\gamma$(keV) | $I_i^\pi \to I_f^\pi$ | $I_\gamma$(%) |
|---|---|---|---|---|---|
| Bands (1) and (2) | | | | | |
| 158.8 | $2^+ \to 0^+$ | 115(6) | 295.4 | $4^+ \to 2^+$ | 100(5) |
| 386.1 | $6^+ \to 4^+$ | 75(5) | 450.7 | $8^+ \to 6^+$ | 45(3) |
| 500.3 | $10^+ \to 8^+$ | 35(2) | 537.2 | $12^+ \to 10^+$ | 18(1) |
| 560.2 | $14^+ \to 12^+$ | 9.2(5) | 576.2 | $16^+ \to 14^+$ | 7.3(4) |
| 601.6 | $18^+ \to 16^+$ | 4.5(3) | 619.7 | $20^+ \to 18^+$ | 2.3(2) |
| 625.8 | $22^+ \to 20^+$ | 0.8(2) | 402.2 | $(9^-) \to (7^-)$ | 2.7(2) |
| 471.1 | $(11^-) \to (9^-)$ | 2.0(2) | 527.0 | $(13^-) \to (11^-)$ | 1.5(2) |
| 574.7 | $(15^-) \to (13^-)$ | 0.9(1) | 617.8 | $(17^-) \to (15^-)$ | 0.22(8) |
| 511.8 | $(7^-) \to 6^+$ | 10.1(6) | 463.3 | $(9^-) \to 8^+$ | 5.7(3) |
| 434.1 | $(11^-) \to 10^+$ | 4.8(3) | 423.9 | $(13^-) \to 12^+$ | 2.3(2) |
| 438.4 | $(15^-) \to 14^+$ | 1.4(2) | 103.1 | $12^+ \to (11^-)$ | 0.82(12) |
| 136.3 | $14^+ \to (13^-)$ | 0.75(10) | 137.8 | $16^+ \to (15^-)$ | 0.3(1) |
| Bands (3) and (4) | | | | | |
| 306.5 | $(5^+) \to (3^+)$ | 8.8(5) | 363.7 | $(7^+) \to (5^+)$ | 7.2(4) |
| 411.8 | $(9^+) \to (7^+)$ | 2.2(2) | 474.7 | $(11^+) \to (9^+)$ | 1.0(1) |
| (195.7) | $(6^-) \to (4^-)$ | | 271.9 | $(8^-) \to (6^-)$ | 4.3(3) |
| 353.3 | $(10^-) \to (8^-)$ | 6.8(6) | 444.3 | $(12^-) \to (10^-)$ | 3.9(3) |
| 536.1 | $(14^-) \to (12^-)$ | 2.2(2) | 611.3 | $(16^-) \to (14^-)$ | 1.2(1) |
| 369.7 | $(4^-) \to (3^+)$ | 8.0(5) | 258.9 | $(6^-) \to (5^+)$ | 8.9(5) |
| 167.1 | $(8^-) \to (7^+)$ | 8.7(4) | 108.6 | $(10^-) \to (9^+)$ | 3.7(2) |
| 104.8 | $(7^+) \to (6^-)$ | 4.8(3) | 244.7 | $(9^+) \to (8^-)$ | 3.3(3) |
| Band (5) $\to$ band (1) | | | | | |
| 306.5 | $(9) \to (7)$ | 3.7(3) | 391.5 | $(11) \to (9)$ | 2.4(2) |
| 482.5 | $(13) \to (11)$ | 1.7(2) | 949.1 | $(7) \to 6^+$ | 5.8(4) |
| 804.9 | $(9) \to 8^+$ | 2.4(2) | 696.1 | $(11) \to 10^+$ | 2.4(2) |
| 641.4 | $(13) \to 12^+$ | 1.2(2) | | | |
| Band (3) $\to$ band (1) | | | | | |
| 958.9 | $(3^+) \to 2^+$ | 10.5(6) | 969.9 | $(5^+) \to 4^+$ | 9.2(5) |
| 663.4 | $(3^+) \to 4^+$ | 7.6(4) | 583.8 | $(5^+) \to 6^+$ | 5.3(3) |
| 947.5 | $(7^+) \to 6^+$ | 5.8(4) | | | |

negative-parity band with odd spin. So the $I^\pi$'s of the band (2) levels are assigned as $(7^-)$, $(9^-)$, $(11^-)$, . . . . A $(7^-)$ instead of $(5^-)$ for the band head is based on the absence of a transition to the $4^+$ level. No other levels below the $7^-$ level were observed in the present work. Above the $10^+$ level where these levels separate more in energy, new $E1$ crossing transitions, 434.1-, 103.1-, 423.9-, 136.3-, 438.4- and 137.8-keV between bands (1) and (2) have been observed, as shown in Fig. 1. Bands (3) and (4) are built on the 1117.6- and 1487.3-keV levels, respectively. Of particular interest is the identification of

TABLE II. Values of internal conversion coefficients ($\alpha_T$) extracted for low energy transitions.

| Nucleus | $E_\gamma$(keV) | $\alpha_T$(Exp.) | $\alpha_T(E1)$ (Theory) | $\alpha_T(M1)$ (Theory) |
|---|---|---|---|---|
| $^{148}$Ce | 104.8($E1$) | 0.20(4) | 0.22 | 1.1 |
| | 108.6($E1$) | 0.16(4) | 0.19 | 1.0 |
| | 167.1($E1$) | 0.044(8) | 0.055 | 0.28 |

the two new linking transitions, 369.7- and 104.8-keV between bands (3) and (4).

Now we examine the spins and parities of the bands (3) and (4). In the early $\beta$-decay measurement [23], the $I^\pi$ of the 1117.6-keV level in band (3) was tentatively assigned as $3^+$ and suggested to be a member of a $\gamma$ band. We concur with this $3^+$ assignment but not the $\gamma$ band assignment. Above the 1117.6-keV level, $I^\pi$'s of the levels in band (3) are assigned as $5^+$, $7^+$, $9^+$ and $11^+$, respectively, based on the regular level spacings.

We have carried out total internal conversion coefficient measurements. The measured total internal conversion coefficients ($\alpha_T$)s' for the three low-energy intertwined transitions 108.6-, 167.1-, and 104.8-keV were used to propose spins and parities to band (4). The $\alpha_T$ for low-energy transitions 108.6-, 167.1-, and 104.8-keV between bands (3) and (4) were determined from the intensity balances in and out of the appropriate levels by double gating on two transitions in the same cascade. The $\alpha_T$ of the 104.8-keV transition (see Fig. 1) was measured by double gating on 258.9- and 353.3-keV transitions. In this gate the difference in relative intensities of
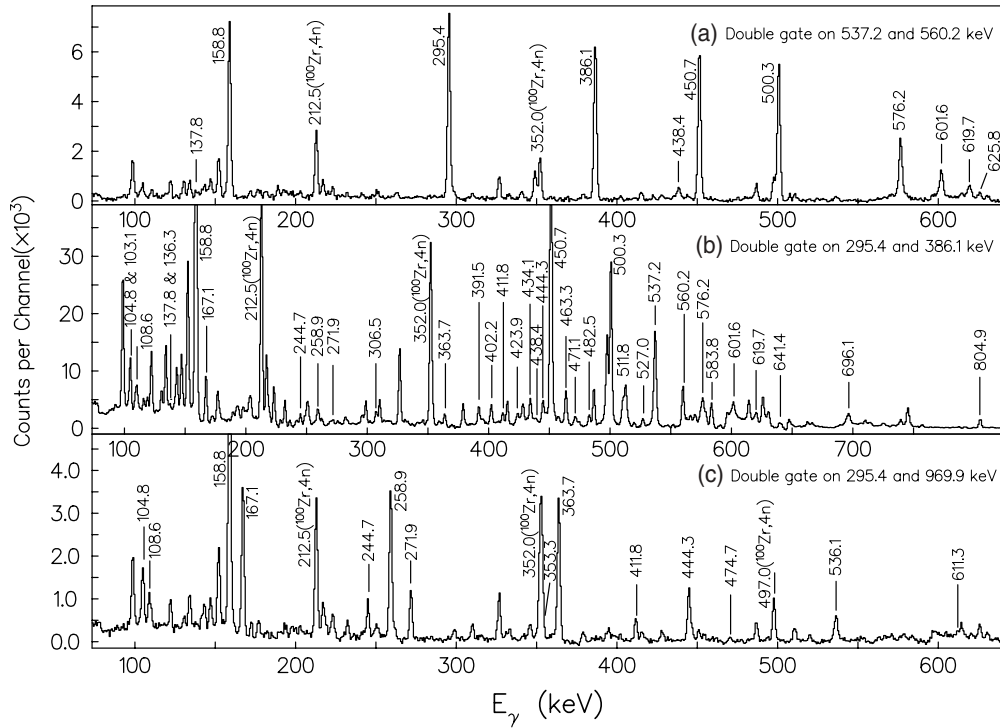
FIG. 2. Partial $\gamma$-ray coincidence spectra obtained by double gating on (a) 537.2- and 560.2-keV, (b) 295.4- and 386.1-keV, and (c) 295.4- and 969.9-keV transitions in $^{148}$Ce. In these three spectra, the transitions belonging to the partner $^{100}$Zr nucleus are indicated.

the 167.1- and 104.8-keV transitions is equal to the conversion electron intensity. By double gating on 947.5- and 108.6-keV transitions, the $\alpha_T$ of the 167.1-keV transition can be extracted, by measuring the difference in relative intensities of the 167.1- and 244.7-keV transitions. In addition, the conversion electron intensity of the 108.6-keV transition (see Fig. 1) equals to the difference in relative intensities of the 444.3-keV and 108.6-keV transitions in a coincidence spectrum obtained by gating on the 244.7-keV and the 536.1-keV transitions.

The three $\alpha_T$ values are listed in Table II. One can see that the measured $\alpha_T$ values of the above low-energy transitions are all in agreement with $E1$ values but not with $M1$ values. Since the three transitions have $E1$ character, there is a change of parity between bands (3) and (4). Thus, band (4) is assigned as the negative-parity band, and the $I^\pi$'s of its levels are tentatively assigned as $4^-, 6^-, 8^-, 10^-, \ldots$, respectively. The $I^\pi$'s of the side band (5) are not clear.

### III. DISCUSSION

From Fig. 1, one can see that two sets of the positive- and negative-parity bands (1) and (2), and bands (3) and (4) with $\Delta I = 2$ transitions in each band and intertwined $E1$ transitions between two bands form a typical octupole band structure and show the reflection asymmetric shape with simplex quantum numbers $s = +1$ and $s = -1$, respectively. Figure 3 shows a comparison of the levels of the $s = +1$ bands in $^{144,146}$Ce [11] and $^{148}$Ce in the present work. As the neutron number increases, the energy of the levels with the same spin decreases.

In order to discuss the octupole deformation stability with spin variation, the energy differences $\delta E$ between the $\pi = +$ and $\pi = -$ bands can be evaluated from the experimental level
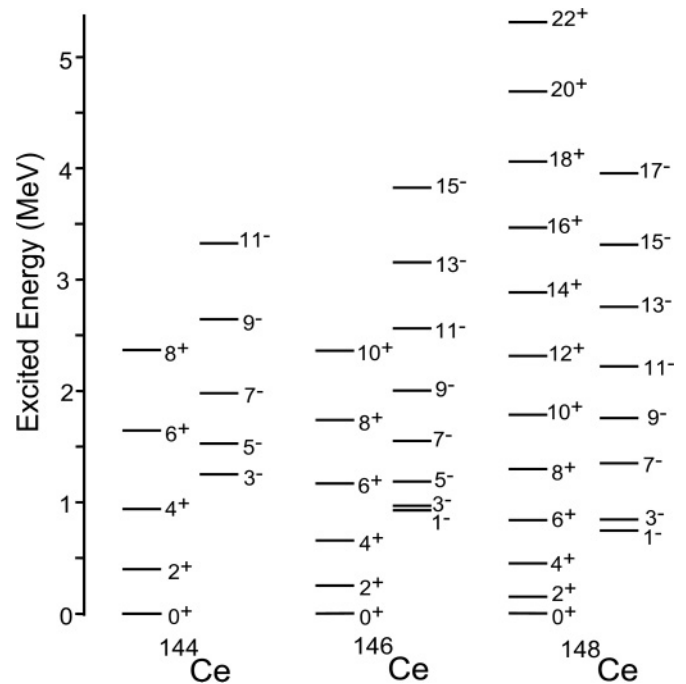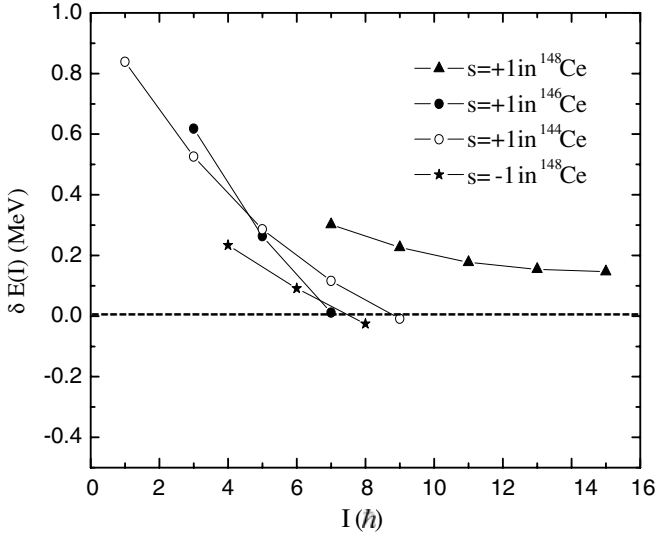


FIG. 3. Systematic comparisons for the levels of $s = +1$ bands in the $^{144,146}$Ce [11] and $^{148}$Ce. The $1^-$ and $3^-$ levels in $^{148}$Ce are taken from Ref. [23].

FIG. 4. Plot of $\delta E(I)$ versus spin $I$.

energies by using the relation [3]

$$\delta E(I) = E(I^-) - \frac{(I+1)E(I-1)^+ + I E(I+1)^+}{2I+1}. \quad (1)$$

Here the superscripts indicate the parities of the levels. Figure 4 compares $\delta E(I)$ versus $I$ curves of $^{148}$Ce and $^{144,146}$Ce. In the limit of stable octupole deformation, $\delta E(I)$ should be close to zero. As seen in Fig. 4, the $\delta E(I)$ decreases and tends towards zero with increasing spin in a way similar to what has been observed in $^{144,146}$Ce especially for the $s=-1$ band of parity doublets. This suggests that the octupole correlation effect observed in $^{148}$Ce is similar to that observed in $^{144,146}$Ce. However, the two bands $s=+1$ and $s=-1$ in $^{148}$Ce show a different behavior: the $s=-1$ band approaches the stable-octupole limit earlier than the $s=+1$ band with increasing spin. The $\delta E(I)$ approaches zero at about $8\hbar$ for the $s=-1$ band. However, from the present data, we can not determine the spin where $\delta E(I)$ for the $s=+1$ band in $^{148}$Ce will approach zero. This may indicate that the octupole correlation in the $s=+1$ band is not as strong as that in the $s=-1$ band.

A nucleus with octupole bands decays through $E1$ and $E2$ transitions. The $B(E1)/B(E2)$ branching ratios are evaluated by the expression

$$\frac{B(E1)}{B(E2)} = 0.771 \frac{I_\gamma(E1)}{I_\gamma(E2)} \frac{E_\gamma(E2)^5}{E_\gamma(E1)^3} (10^{-6} \text{ fm}^{-2}), \quad (2)$$

where the intensities ($I_\gamma$) and energies ($E_\gamma$) have been taken from the present work. The $B(E1)/B(E2)$ values in $s=\pm1$ bands of $^{148}$Ce from our investigation are listed in Table III. The average $B(E1)/B(E2)$ value is $0.82 \times (10^{-6} \text{ fm}^{-2})$ for the $s=+1$ band, and $1.51 \times (10^{-6} \text{ fm}^{-2})$ for the $s=-1$ band. These values are comparable (an order of magnitude) with the neighboring isotopes $^{144,146}$Ce [11]. Indeed, strong $E1$ transitions between the positive-parity and negative-parity bands are seen, and indicate that the octupole correlation in $^{148}$Ce is strong. The average $B(E1)/B(E2)$ value for the $s=-1$ band is larger than that for the $s=+1$ band. This may imply that the octupole correlations are stronger for the $s=-1$

TABLE III. $B(E1)/B(E2)$ branching ratios in $^{148}$Ce.

| | $E_\gamma$(keV) | $I_i^\pi \to I_f^\pi$ | $I_\gamma$ | $\frac{B(E1)}{B(E2)} 10^{-6}$ fm$^{-2}$ |
|---|---|---|---|---|
| $s=-1$ | 104.8 | $(7^+) \to (6^-)$ | 4.8 | 2.8(5) |
| | 363.7 | $(7^+) \to (5^+)$ | 7.2 | |
| | 167.1 | $(8^-) \to (7^+)$ | 8.7 | 0.5(1) |
| | 271.9 | $(8^-) \to (6^-)$ | 4.3 | |
| | 244.7 | $(9^+) \to (8^-)$ | 3.3 | 0.94(13) |
| | 411.8 | $(9^+) \to (7^+)$ | 2.2 | |
| | 108.6 | $(10^-) \to (9^+)$ | 3.7 | 1.8(4) |
| | 353.3 | $(10^-) \to (8^-)$ | 6.8 | |
| $s=+1$ | 463.3 | $(9^-) \to 8^+$ | 5.7 | 0.17(4) |
| | 402.2 | $(9^-) \to (7^-)$ | 2.7 | |
| | 434.1 | $(11^-) \to 10^+$ | 4.8 | 0.53(7) |
| | 471.1 | $(11^-) \to (9^-)$ | 2.0 | |
| | 103.1 | $12^+ \to (11^-)$ | 0.82 | 1.42(24) |
| | 537.2 | $12^+ \to 10^+$ | 17.6 | |
| | 423.9 | $(13^-) \to 12^+$ | 2.3 | 0.63(14) |
| | 527.0 | $(13^-) \to (11^-)$ | 1.5 | |
| | 136.3 | $14^+ \to (13^-)$ | 0.75 | 1.34(20) |
| | 560.2 | $14^+ \to 12^+$ | 9.2 | |
| | 438.4 | $(15^-) \to 14^+$ | 1.4 | 0.89(16) |
| | 574.7 | $(15^-) \to (13^-)$ | 0.9 | |
| | 137.8 | $16^+ \to (15^-)$ | 0.3 | 0.77(27) |
| | 576.2 | $16^+ \to 14^+$ | 7.3 | |

band than that for the $s=+1$ band as also indicated by the $\delta E(I)$ values in Fig. 4. The similar situation is observed in $^{143}$Ba [8], where the average $B(E1)/B(E2)$ value for the $s=-i$ band is much larger than that for the $s=+i$ band.

Plots of the kinematic moments of inertia ($J_1$) against $\hbar\omega$ for the $s=\pm1$ bands in $^{148}$Ce as well as the $s=+1$ band in $^{146}$Ce are shown in Fig. 5. The $J_1$ values of the negative-parity bands are much larger than those in their positive-parity bands at low $\hbar\omega$ values in each pair of the parity doublet bands. The smoothly increasing trends of $J_1$ with $\hbar\omega$ for the $s=+1$ bands in $^{148}$Ce and $^{146}$Ce are very similar until the upbend in
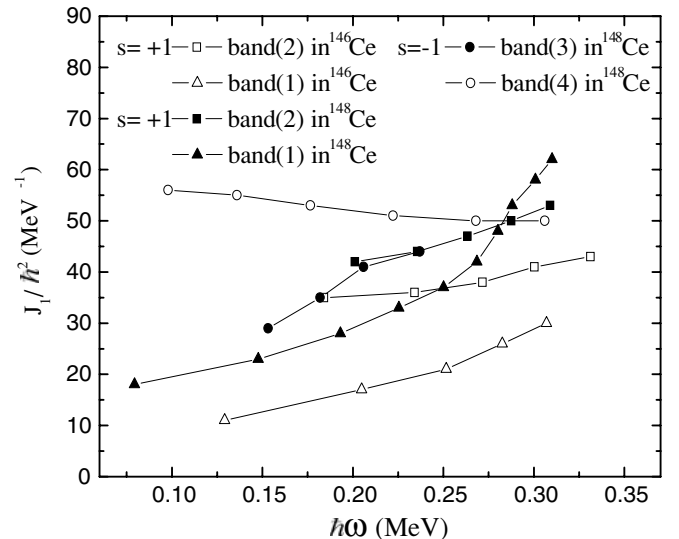


FIG. 5. Moments of inertia ($J_1$) for bands in $^{148}$Ce and $^{146}$Ce.

$^{148}$Ce around $12^+$. This also implies that the $s = +1$ band in $^{148}$Ce is similar in structure to the $s = +1$ bands in $^{144,146}$Ce. However, for the $s = -1$ band in $^{148}$Ce, we see that the $J_1$ of the negative-parity band [band (4)] smoothly decreases as $\hbar\omega$ increases, but the $J_1$ of the positive-parity band [band (3)] smoothly increases as $\hbar\omega$ increases. Such a different variations of the $J_1$ values with $\hbar\omega$ for the two branches of an octupole deformation band also are seen in the $s = -i$ band in $^{145}$Ba [8]. The different $J_1$ values in bands (1)–(4) of $^{148}$Ce may suggest that the octupole deformation may not be stable, as discussed in $^{145}$La [13]. This structural feature calls for more theoretical work. In addition, one can see that band (1) in $^{148}$Ce shows a sharp upbend beginning at the $14^+ \rightarrow 12^+$ transition that is not seen in band (2). This sharp upbend in the yrast band (1) might be caused by alignment of a pair of protons or neutrons.

## IV. SUMMARY

In the present work, we have investigated the band structure of $^{148}$Ce and identified both the $s = +1$ and $s = -1$ octupole correlated bands in $^{148}$Ce. We not only observed the first evidence for $E1$ transitions intertwined with the $^{148}$Ce yrast cascade, but also observed new side bands in $^{148}$Ce which show a strong octupole structure with the simplex quantum number $s = -1$. The measured $\alpha_T$ values for some low-energy intertwined transitions support this conclusion. This is the first report of an $s = -1$ octupole deformation structure in the neutron-rich Ce isotopes. The $B(E1)/B(E2)$ branching ratios indicate that the octupole correlations in $^{148}$Ce are stronger for the $s = -1$ band than that for the $s = +1$ band.

[1] W. Nazarewicz, P. Olanders, I. Ragnarsson, J. Dudek, and G. A. Leander, Phys. Rev. Lett. **52**, 1272 (1984).

[2] W. Nazarewicz, P. Olanders, I. Ragnarsson, J. Dudek, G. A. Leander, P. Moller, and E. Ruchowska , Nucl. Phys. **A429**, 269 (1984).

[3] W. Nazarewicz and P. Olanders, Nucl. Phys. **A441**, 420 (1985).

[4] W. Nazarewicz, G. A. Leader, and J. Dudek, Nucl. Phys. **A467**, 437 (1987).

[5] J. H. Hamilton, A. V. Ramayya, S. J. Zhu, G. M. Ter-Akopian, Yu. Ts. Oganessian, J. D. Cole, J. O. Rasmussen, and M. A. Stoyer, Prog. Part. Nucl. Phys. **35**, 635 (1995).

[6] S. J. Zhu, Q. H. Lu, J. H. Hamilton, A. V. Ramayya, L. K. Peker, M. G. Wang, W. C. Ma, B. R. S. Babu, T. N. Ginter, J. Kormicki, D. Shi, J. K. Deng, W. Nazarewicz, J. O. Rasmussen, M. A. Stoyer, S. Y. Chu, K. E. Gregorich, M. F. Mohar, S. Asztalos, S. G. Prussin, J. D. Cole, R. Aryaeinejad, Y. K. Dardenne, M. Drigert, K. J. Moody, R. W. Loughed, J. F. Wild, N. R. Johnson, I. Y. Lee, F. K. McGowan, G. M. Ter-Akopian, and Yu. Ts. Oganessian, Phys. Lett. **B357**, 273 (1995).

[7] M. A. Jones, W. Urban, J. L. Durell, M. Leddy, W. R. Phillips, A. G. Smith, B. J. Varley, I. Ahmad, L. R. Morss, M. Bentaleb, E. Lubkiewicz, and N. Schulz, Nucl. Phys. **A605**, 133 (1996).

[8] S. J. Zhu, J. H. Hamilton, A. V. Ramayya, E. F. Jones, J. K. Hwang, M. G. Wang, X. Q. Zhang, P. M. Gore, L. K. Peker, G. Drafta, B. R. S. Babu, W. C. Ma, G. L. Long, L. Y. Zhu, C. Y. Gan, L. M. Yang, M. Sakhaee, M. Li, J. K. Deng, T. N. Ginter, C. J. Beyer, J. Kormicki, J. D. Cole, R. Aryaeinejad, M. W. Drigert, J. O. Rasmussen, S. Asztalos, I. Y. Lee, A. O. Macchiavelli, S. Y. Chu, K. E. Gregorich, M. F. Mohar, G. M. Ter-Akopian, A. V. Daniel, Yu. Ts. Oganessian, R. Donangelo, M. A. Stoyer, R. W. Loughed, K. J. Moody, J. F. Wild, S. G. Prussin, J. Kliman, and H. C. Griffin, Phys. Rev. C **60**, 051304(R) (1999).

[9] W. R. Phillips, I. Ahmad, H. Emling, R. Holzmann, R. V. F. Janssens, T. L. Khoo, and M. W. Drigert, Phys. Rev. Lett. **57**, 3257 (1986).

[10] W. R. Phillips, R. V. F. Janssens, I. Ahmad, H. Emling, R. Holzmann, T. L. Khoo, and M. W. Drigert, Phys. Lett. **B212**, 402 (1988).

[11] L. Y. Zhu, S. J. Zhu, M. Li, J. H. Hamilton, A. V. Ramayya, B. R. S. Babu, W. C. Ma, J. O. Rasmussen, M. A. Stoyer, and I. Y. Lee, High Energy Phys. Nucl. Phys.-Chinese Edition **22**(10), 885 (1997).

[12] W. Urban, W. R. Phillips, J. L. Durell, M. A. Jones, M. Leddy, C. J. Pearson, A. G. Smith, B. J. Varley, I. Ahmad, L. R. Morss, M. Bentaleb, E. Lubkiewicz, and N. Schulz, Phys. Rev. C **54**, 945 (1996).

[13] S. J. Zhu, J. H. Hamilton, A. V. Ramayya, M. G. Wang, J. K. Hwang, E. F. Jones, L. K. Peker, B. R. S. Babu, G. Drafta, W. C. Ma, G. L. Long, L. Y. Zhu, M. Li, C. Y. Gan, T. N. Ginter, J. Kormicki, J. K. Deng, D. T. Shi, W. E. Collins, J. D. Cole, R. Aryaeinejad, M. W. Drigert, J. O. Rasmussen, R. Donangelo, J. Gilat, S. Asztalos, I. Y. Lee, A. O. Macchiavelli, S. Y. Chu, K. E. Gregorich, M. F. Mohar, M. A. Stoyer, R. W. Loughed, K. J. Moody, J. F. Wild, S. G. Prussin, G. M. Ter-Akopian, A. V. Daniel, and Yu. Ts. Oganessian, Phys. Rev. C **59**, 1316 (1999).

[14] P. A. Butler and W. Nazarewicz, Phys. Rev. Mod. Phys. **68**, 349 (1996).

[15] W. Urban, R. M. Lieder, J. C. Bacelar, P. P. Singh, D. Alber, D. Balabanski, W. Gast, H. Grawe, G. Hebbinghaus, J. R. Jongman, T. Morek, R. F. Noorman, T. Rzaca-Urban, H. Schnare, M. Thomas, O. Zell, and W. Nazarewicz, Phys. Lett. **B258**, 293 (1991).

[16] V. E. Iacob, W. Urban, J. C. Bacelar, J. Jongman, J. Nyberg, G. Sletten, and L. Trache, Nucl. Phys. **A596**, 155 (1996).

[17] W. Nazarewicz and S. L. Tabor, Phys. Rev. C **45**, 2226 (1992).

[18] J. L. Egido and L. M. Robledo, Nucl. Phys. **A545**, 589 (1992).

[19] W. Urban, T. Rzaca-Urban, W. R. Phillips, J. L. Durell, M. J. Leddy, A. G. Smith, B. J. Varley, N. Schulz, M. Bentaleb, E. Lubkiewicz, I. Ahmad, and L. R. Morss, in *Proceedings of the International Conference on Fission*, edited by J. H. Hamilton, W. R. Phillips, and H. K. Carter (World Scientific press, Singapore, 1999), p. 136.

[20] S. J. Zhu, C. Y. Gan, J. H. Hamilton, A. V. Ramayya, B. R. S. Babu, M. Sakhaee, W. C. Ma, G. L. Long, J. K. Deng, L. Y. Zhu, M. Li, L. M. Yang, J. Komicki, J. D. Cole, R. Aryaeinejad, Y. K. Dardenne, M. W. Drigert, J. O. Rasmussen, M. A. Stoyer, S. Y. Chu, K. E. Gregorich, M. F. Mohar, S. G. Prussin, I. Y. Lee, N. R. Johnson, and K. F. McGowan, Chin. Phys. Lett. **15**, 793 (1998).

[21] D. C. Radford, Nucl. Instrum. Methods Phys. Res. A **361**, 297 (1995).

[22] S. J. Zhu, J. H. Hamilton, A. V. Ramayya, J. K. Hwang, C. Y. Gan, X. Q. Zhang, C. J. Beyer, J. Kormicki, M. Sakhaee, L. M. Yang, L. Y. Zhu, R. Q. Xu, Z. Zhang, Z. Jiang, W. C. Ma, E. F. Jones, P. M. Gore, J. D. Cole, M. W. Drigert, I. Y. Lee, J. O. Rasmussen, T. N. Ginter, Y. X. Luo, S. C. Wu, C. Folden, P. Fallon, P. Zielinski, K. E. Gregorich, A. O. Macchiavelli, S. J. Asztalos, G. M. Ter-Akopian, Yu. Ts. Oganessian, M. A. Stoyer, J. P. Greene, R. V. F. Janssens, and I. Ahmad, Phys. Rev. C **65**, 014307 (2001).

[23] R. L. Gill, M. Shmid, R. E. Chrien, Y. Y. Chu, A. Wolf, D. S. Brenner, K. Sistemich, F. K. Wohn, H. Yamamoto, C. Chung, and W. B. Walters, Phys. Rev. C **27**, 1732 (1983).